EBioMedicine 41 (2019) 670–682

Contents lists available at ScienceDirect

EBioMedicine

journal homepage: www.ebiomedicine.com

EBioMedicine
Published by THE LANCET

miR-4739 mediates pleural fibrosis by targeting bone morphogenetic protein 7

Meng Wang [a,1], Liang Xiong [b,c,1], Li-Juan Jiang [b], Yu-Zhi Lu [b], Fei Liu [a], Lin-Jie Song [b,c], Fei Xiang [b,c], Xin-Liang He [b,c], Fan Yu [b,c], Shi-Yuan Shuai [b,c], Wan-Li Ma [b,c,*], Hong Ye [a,c,**]

[a] Department of Pathophysiology, School of Basic Medicine, Tongji Medical College, Huazhong University of Science and Technology, Wuhan 430022, China
[b] Department of Respiratory and Critical Care Medicine, Union Hospital, Tongji Medical College, Huazhong University of Science and Technology, Wuhan 430022, China
[c] Key Laboratory of Respiratory Diseases, Ministry of Health of China, Wuhan 430030, China

ARTICLE INFO

Article history:
Received 19 November 2018
Received in revised form 20 February 2019
Accepted 26 February 2019
Available online 5 March 2019

Keywords:
Pleural fibrosis
Pleural mesothelial cells (PMCs)
miR-4739
BMP-7
Mesothelial-mesenchymal transition (MMT)

ABSTRACT

Background: Pleural fibrosis is defined as excessive depositions of matrix components that result in pleural tissue architecture destruction and dysfunction. In severe cases, the progression of pleural fibrosis leads to lung entrapment, resulting in dyspnea and respiratory failure. However, the mechanism of pleural fibrosis is poorly understood.

Methods: miR-4739 levels were detected by miRNA array and real-time PCR. Real-time PCR, western blotting and immunofluorescence were used to identify the expression profile of indicators related to fibrosis. Target gene of miR-4739 and promoter activity assay was measured by using dual-luciferase reporter assay system. In vivo, pleural fibrosis was evaluated by Masson staining and miR-4739 level was detected by In situ hybridization histochemistry.

Findings: We found that bleomycin induced up-regulation of miR-4739 in pleural mesothelial cells (PMCs). Over-regulated miR-4739 mediated mesothelial-mesenchymal transition and increased collagen-I synthesis in PMCs. Investigation on the clinical specimens revealed that high levels of miR-4739 and low levels of bone morphogenetic protein 7 (BMP-7) associated with pleural fibrosis in patients. Then we next identified that miR-4739 targeted and down-regulated BMP-7 which further resulted in unbalance between Smad1/5/9 and Smad2/3 signaling. Lastly, in vivo studies revealed that miR-4739 over-expression induced pleural fibrosis, and exogenous BMP-7 prevented pleural fibrosis in mice.

Interpretation: Our data indicated that miR-4739 targets BMP-7 which mediates pleural fibrosis. The miR-4739/BMP-7 axis is a promising therapeutic target for the disease.

Fund: The National Natural Science Foundation of China.

1. Intruduction

The lungs and inner surface of the thoracic wall are covered by an elastic, serous and lubricating membrane to form the pleural cavity. It is named pleura. The pleura act not only as a protective barrier but as an immunologically and metabolically responsive membrane. In the pathological process, damages of normal pleura mediate inflammation, fibrosis and even tumorigenesis [1].

Pleural fibrosis is defined as excessive depositions of matrix components that result in pleural tissue architecture destruction and dysfunction. It can be a result of various inflammatory processes such as tuberculous pleurisy, bacterial empyema, rheumatoid pleurisy, asbestos exposure, retained hemot horax and medications [2,3]. Pleural fibrosis leads to clinical events such as cough and dyspnea, even respiratory failure and death [4]. Similar to other fibrosis diseases, the pathological process of pleural fibrosis is irreversible, and pleural decortication is eventually the only treatment option.

The pleura is lined by a monolayer of pleural mesothelial cells (PMCs) which rest on a thin basement membrane supported by connective tissue, fibroblast-like cells, blood and lymphatic vessels. PMCs play important roles in fluid and cell transport, initiation and resolution of inflammation, tissue repair, lysis of fibrin deposits preventing adhesion formation and protection against invading microorganisms, and possibly tumor dissemination [5]. Studies have revealed that the response

* Correspondence to: W.-L. Ma, Department of Respiratory and Critical Care Medicine, Union Hospital, Tongji Medical College, Huazhong University of Science and Technology, 1277 JieFang Avenue, Wuhan 430022, PR China.
** Correspondence to: H. Ye, Department of Pathophysiology, School of Basic Medicine, Tongji Medical College, Huazhong University of Science and Technology, 13 Hang Kong Road, Wuhan 430030, PR China.
E-mail addresses: whmawl@aliyun.com (W.-L. Ma), yehmwl@hust.edu.com (H. Ye).
[1] These authors contributed equally to this work.

https://doi.org/10.1016/j.ebiom.2019.02.057

Research in context

Evidence before this study

Pleural fibrosis is a common disorder followed exudative pleural effusion. In severe cases, the progression of pleural fibrosis leads to lung entrapment, resulting in dyspnea and respiratory failure. However, the mechanism of pleural fibrosis is poorly understood. Moreover, pleural decortication is eventually the only treatment option, and new strategy for pleural fibrosis therapy is urgently needed.

Added value of this study

Here, it is first report that up-regulation of miR-4739 in pleural mesothelial cells (PMCs) mediated the pleural fibrosis, and the related mechanism is that miR-4739 targeted and down-regulated BMP-7 which further resulted in unbalance between Smad1/5/9 and Smad2/3 signaling.

Implications of all the available evidence

The present work indicates that up-regulated miR-4739 mediated pleural fibrosis. The miR-4739/BMP-7 axis is a promising therapeutic target for pleural fibrosis.

of PMCs to injury and the ability to maintain its integrity play a pivotal role in the pleural fibrotic process [6–8]. We previously reported that the PMC polarity changed and produced an excess of collagen-I which contributed to pleural fibrosis [9,10]. However, the detailed mechanism is still poorly understood.

microRNAs (miRNAs) are endogenous short non-coding RNA molecule (about 22 bp) with single stranded and evolutionarily conserved sequences [11–13]. Approximately 10% of miRNAs in the lungs of idiopathic pulmonary fibrosis patients show significant deregulation [14], and the role of miRNA in the pathogenesis of pulmonary fibrosis has received considerable attention. However, to our best knowledge, there is no literature referred to the role of miRNAs in pleural fibrosis. It is known that epithelial cells undergoing epithelial-mesenchymal transition (EMT) play an important role in fibrotic disease [2,15,16]. As the epithelial-like cells, PMCs can undergo EMT which is also named mesothelial-mesenchymal transition (MMT) [2,9,17]. PMCs with MMT are considered as a source of myofibroblasts which contributed to deposition of ECM in fibrosis [9,18,19]. Thus, the relationships of miRNAs, PMC-MMT and pleural fibrosis imperatively need clarification.

The transforming growth factor-β (TGF-β) super-family consists of >33 proteins which could be secreted out of the cells as homodimers or heterodimers [20]. The super-family members include TGF-βs, bone morphogenetic proteins (BMPs), activins and inhibins. These members participate in biological processes by binding with different sets of heteromeric type I and type II receptor, and then activate Smad or non-Smad signaling [21]. In different stages of growth, development and disease, TGF-β super-family has been confirmed to play a crucial role [22–24]. TGF-β1, as the most important one in TGF-β super-family, could induce the phenotypic transformation of mesenchymal origin cells through Smad2 and Smad3 signaling [25]. TGF-β1-Smad2/3 pathway has been confirmed to mediate different fibrotic diseases [26–28]. BMPs are multi-functional growth factors belong to the TGF-β super-family [29], and BMPs-Smad1/5/9 pathway and its inhibitors are also important to maintain the normal physiological development [30]. It keeps a balance between TGF-β1 and BMPs signaling, but in fibrotic diseases of kidney, lung and retina, the balance is broken [31–33]. In most cases, TGF-β1 signaling increased and some BMPs signaling decreased [34]. It still unknown whether BMPs mediate pleura fibrosis. Bleomycin is widely used as an inducer in animal models of pulmonary fibrosis. Decologne and colleagues successfully made pleural fibrosis animal model by using bleomycin in the presence of carbon particles in 2010 [35]. We recently reported that bleomycin induced MMT of PMCs through TGF-β1-Smad2/3 signaling which resulted in sub-pleural fibrosis [9]. In the current study, to explore the mechanism of pleural fibrosis we used bleomycin in cell experiments and animal models. Using miRNA microarray analysis, we found some miRNAs changed in PMCs treated by bleomycin, and miR-4739 was one of the most obviously changed miRNAs. And in our cellular preliminary experiment, over-expression of miRNA-4739 (miR-4739) induced significant increases in collagen-I which was the sign of fibrosis. Then we made hypothesis that miR-4739 is involved in the pleural fibrosis. Thus, the aim of the study is to disclose the role of miR-4739 in pleural fibrosis, and the underling mechanism especially which concerned TGF-β and BMP signaling.

2. Materials and methods

2.1. Reagents and antibodies

TGF-β1 was purchased from Sigma-Aldrich Corp (St. Louis, MO, USA). TGF-β1 receptor inhibitor (SB431542) was obtained from R&D Systems (Minneapolis, MN, USA). Recombinant human BMP-7 protein was purchased from NovusBiologicals (Littleton, CO, USA). Carbon particles were purchased from Mitsubishi Chem5-ical Corporation (Tokyo, Japan). Bleomycin was purchased from Tianjin Taihe Pharmaceutical Co., Ltd. (Tianjin, China). Antibodies against collagen-I (Cat#14695-1-AP), BMP-7 (Cat#12221-1-AP), α-smooth muscle actin (α-SMA) (Cat#55135-1-AP), TGF-β1 (Cat#21898-1-AP) and GAPDH (Cat#60004–1-lg) were purchased from Proteintech (Rosemont, IL, USA). Anti-E-cadherin antibody (Cat#14472), Anti-phospho-Smad2/3 (p-Smad2/3) (Cat#8828) antibody, Anti-phospho-Smad1/5/9 (p-Smad1/5/9) (Cat#13820) antibody, Anti-total-Smad2/3 (t-Smad2/3) (Cat#8685) antibody, Flag Tag (Cat#14793) and HA Tag (Cat#3724), were purchased from Cell Signaling Technology (Danvers, MA, USA). Antibodies against vimentin (Cat#2707-1) and cytokeratin-8 (Cat#2032-1) were purchased from Epitomics (Burlingame, CA, USA). Anti-total-Smad1 (t-Smad1) (Cat#A1101) and Anti-Snail1 (Cat#A5243) antibody was purchased from ABclonal (Woburn, MA, USA). Antibody against Wilms tumor 1 (Wt1) (Cat#NB110–60011) was purchased from NovusBiologicals. Antibody against calretinin (Cat#610908) was purchased from BD Bioscience (Franklin Lakes, NJ, USA).

2.2. Plasmid construct

The expression vectors of Smad1 and Smad3 were sub-cloned into pCMV-C-HA plasmid. Smad1 was PCR-amplified and inserted between the *Sal*I and Bg1II sites, and Smad3 was inserted between the *Eco*RI and *Xho*I sites. The expression vectors of Smad4 were sub-cloned into pENTER-C-Flag plasmid. Smad4 was inserted between the AsisI and M1uI sites. All constructs were sequence-checked.

2.3. PMCs culture

The human PMCs line MeT-5A which was SV40-transformed was purchased from the American Type Culture Collection (ATCC, Manassas, VA, USA). The cells were sub-cultured at 1:3 ratios when cells grew to confluence, and culture medium was changed every 2 days. Cells equilibrated overnight were used for all experiments.

2.4. Isolation, identification and primary culture of rat primary PMCs

Rat primary PMCs were isolated from rat pleura with protease as our previous studies [10,36]. In brief, the whole thorax was isolated under

sterile conditions after 1 mg/ml protease from streptomyces griseus (Sigma) in 5 ml RPMI-1640 medium injected into thoracic cavity and then digested at 4 °C overnight. The cells were harvested and centrifuged at 1, 000 rpm for 5 min (min). The spun down cells were resuspended in epithelial cell medium-animal (ScienCell, Carlsbad, CA, USA) and incubated for 7 days and then replaced with RPMI-1640 containing 20% FBS. Other treatments were the same as with Met-5A cells. To confirm the phenotype of the rat primary PMCs, the isolated cells were incubated with antibodies against Wt1 (dilution 1:50) and calretinin (dilution 1:50) at 4 °C overnight. The Cy3- or FITC-labeled secondary antibody immunoglobulin G (IgG) (ABclonal) was added and incubated for 30 min. The nucleus was stained for DAPI for 10 min in the dark. Labeled cells were examined using a fluorescence microscope (Olympus FV500, Olympus, Tokyo, Japan).

2.5. Isolation and identification of human primary PMCs from pleural effusion

The fresh pleural effusion was initially filtered with gauze to remove larger impurity. Then the cells were harvested and centrifuged at $1500 \times g$ for 6 min at 4 °C. The precipitated cells were used to extracted protein and mRNA. To confirm the phenotype of the human primary PMCs, the precipitated cells were planted on the glass slide and incubated with antibodies against calretinin (dilution 1:50) at 4°C overnight. The Cy3-labeled secondary antibody IgG (ABclonal) was added and incubated for 30 min. The nucleus was stained for DAPI for 10 min in the dark. Labeled cells were examined using a fluorescence microscope.

2.6. Quantification of miR-4739

Total cellular RNA was extracted by using TRIzolreagent. miR-cDNAs were synthesized by using the One Step PrimeScript miRNA cDNA Synthesis Kit (Takara Bio Inc., Kusatsu, Japan). miR-cDNAs amplified by real-time PCR using SYBR Premix EX Taq II Kit (Takara Bio Inc., Kusatsu, Japan). miR-4739 expression was normalized with U6. The primers of miR-4739 and U6 were obtained from Qiagen (Hilden, Germany).

2.7. miR-4739 over-expression and inhibition

miR-4739 over-expression was acquired employing recombinant lentivirus encoding miR-4739. Inhibition of miR-4739 was achieved employing recombinant lentivirus encoding a siRNA targeted against miR-4739 (siRNA sequence 5'-AGGGCCCCTCCGCTCCTC CTCCCTT-3′). All the recombinant lentivirus including control recombinant lentivirus (control sequence 5′- TTCTCCGAACGTGTCACGT-3′) were provided by Genechem (Shanghai, China). Transfection of cells with lentiviruses was performed according to the manufacturer's instructions. Cells were incubated in CO_2 incubator for 8 h (h), and the medium was then replaced with fresh RPMI-1640 containing 20% FBS. Transfection efficiency was evaluated by GFP reporter gene by fluorescence microscopy.

2.8. Bleomycin-induced pleural fibrosis model and treatments

All animal experiments were performed in accordance with the Guide for the Care and Use of Laboratory Animals and approved by the Institutional Animal Care and Use Committee (IACUC) of the Tongji Medical College, Huazhong University of Science and Technology. Specific-pathogen-free 6–8 weeks old male C57BL/6J mice were maintained under specific-pathogen-free conditions. A mixture of bleomycin (0.48 μg/mouse) and carbon particles (0.1 mg/mouse) was administered in a volume of 100 μl 0.9% NaCl by intrapleural injection on the right side with a 22-G needle. Mice in the control group were received intrapleural injection with 100 μl 0.9% NaCl. Some mice were intraperitoneally injected with 150 μg/kg BMP-7 at 4, 7, 10 days. All mice were euthanized after 21 days, and the tissues were taken for histological analysis.

2.9. miR-4739 over-expression in mice

Male C57BL/6J mice (age 6–8 weeks) were divided into three groups (normal control, vector control and miR-4739 over-expression). Mice in the normal control group were intrapleural injected with 0.9% NaCl. Intrapleural injection of carbon particles (0.1 mg/mouse) and control lentivirus (2×10^6 TU/mouse) was administrated in the vector control group at days 1, 5 and 8. Mice in miR-4739 over-expression group were intrapleural injected with carbon particles (0.1 mg/mouse) and lentivirus expressing miR-4739 (2×10^6 TU/mouse) at the same times. Some mice in miR-4739 over-expression group were intraperitoneally injected with 150 μg/kg BMP-7 or miR-4739 inhibition lentivirus (2×10^6 TU/mouse) at days 11, 14 and 17. All mice were euthanized after 21 days, and the tissues were taken for histological and immunofluorescence staining.

2.10. Enzyme-linked immunosorbent assay (ELISA)

The amount of TGF-β1 in PMC culture medium was measured by using a human TGF-β1 ELISA kit from R&D Systems. The procedures were performed according to the manufacturer's instruction.

2.11. Reverse transcription-quantitative polymerase chain reaction (RT-qPCR) analysis

Total cellular RNA was extracted using TRIzolreagent. RNA levels of collagen-I, E-cadherin, cytokeratin-8, vimentin, α-SMA and primary miR-4739 (pri-miR-4739) mRNA were determined by RT-qPCR. PCR ran under the following conditions after the total RNA reverse transcribed:95 °C for 30 s, 40 cycles of 95 °C for 10 s, and 60 °C for 20 s. The pri-miR-4739 PCR primer was: 5′-GCTGGGACATTGAAAGTCTCA-3′, forward; 5′-GATGTTCCCATCGGCGTGTC-3′, reverse. Other primers we used were same as our previous research [37]. The results were expressed as $2^{-\Delta\Delta T}$ using GAPDH as a reference.

2.12. Western blot analysis

Cell lysates were denatured and electrophoresed on SDS-PAGE gel. The primary antibodies were antibody against collagen-I (dilution 1:1000), E-cadherin (dilution 1:1000), cytokeratin-8 (dilution 1:2000), vimentin (dilution 1:2000), α-SMA (dilution 1:1000), Snail1 (dilution 1:1000), p-Smad2/3 (dilution 1:400), t-Smad2/3 (dilution 1:1000), p-Smad1/5/9 (dilution 1:300), t-Smad1(dilution 1:1000), BMP-7 (dilution 1:1000), and GAPDH (dilution 1:10000). HRP labeled secondary antibody IgG (ABclonal) was diluted in TTBS plus 5% nonfat milk and incubated with the membrane at room temperature for 1 h. At last, films were developed by using Kodak Medical X-ray processor 102 (Kodak, Rochester, NY, USA) and ChemiDoc MP Imager (Bio-Rad, Redmond, WA, USA) to visualize the reactive proteins followed by densitometric quantification using Image-Pro Plus software (Media Cybernetics, Rockville, MD, USA).

2.13. Wound-healing assay of PMC migration

As previously reported, cells were seeded into six-well plates and then scratched using the tip of a p-200 pipette to create a uniform cell-free zone in each well [38]. The scratched cells were removed by PBS for three times. Wounded monolayers were then incubated with the indicated conditions. Microscopic images were taken with a digital camera at different time points after wounding. The recovered area was measured by using the Image-Pro Plus software and expressed as a percentage of the initial scratched area.

2.14. Cell proliferation assay

Cell proliferation assay was performed as previously described [39]. PMCs collected in the logarithmic phase were plated into 96-well plates (2×10^3 cells/well). Cell Counting Kit-8 (Dojindo, Kumamoto, Japan) was used according to the manufacturer's instruction.

2.15. Target gene of miR-4739 assay

The 211-nt sequences of the human (NM_001719) and rat (NM_001191856) wild-type BMP-7 3'UTR containing the predicted seed binding sequence for miR-4739 (CCTCCCT) and (CCTCCC) were synthesized, and sub-cloned into pMIR-Report luciferase. The controls were generated with mutation of the miR-4739 binding sequence in the human BMP-7 3' UTR that changed the seed binding sequence to ATGAGTC, and changed the rat BMP-7 3'UTR seed sequence to ATGA GT. miR-4739 over-expression was established by transfecting HEK293T cells with lentivirus expressing miR-4739. Cells were then seeded in 6-well plates at 80% confluence and transfected with 2 μg per well of human pMIR-wt-BMP-7-3'UTR or pMIR-mut-BMP-7-3'UTR vectors, and rat pMIR-wt-BMP-7-3'UTR or pMIR-mut-BMP-7-3'UTR vectors by lipofectamine 2000 (Invitrogen, Carlsbad, CA, USA). All cells also transfected with renilla luciferase plasmid at same time. Cells were harvested after 24 h, and luciferase activity was measured by using a dual-luciferase reporter assay system (Promega, Madison, WI, USA) with a Synergy 2 Multi-Mode microplate reader. Relative expression of firefly and renilla luciferase was calculated.

2.16. Promoter activity assay

The promoter of E-cadherin reporter was subcloned into pGL3-basic plasmid. The 2520-nt sequence before the transcription start site (TSS) was PCR-amplified and inserted between the M1uI and Bg1II sites, and the 2540-nt sequence of Col1a1 promoter was inserted between the *Kpn*I and M1uI sites. The location of the theoretical transcription start site (TSS) and proximal promoter region of the miR-4739 in chromosome 17 was predicted by the miRTrans (http://mcube.nju.edu.cn/jwang/lab/soft/mirtrans/) [40]. According to miRTrans, we selected the two location (chr17:797288551:-, chr17:79741814:-) as the TSSs. Then the promoter of pri-miR-4739 reporter gene was subcloned into pGL3-basic plasmid. The two 1000-nt sequences before the TSSs were synthesized and inserted between the *Kpn*I and *Xho*I sites. Cells were seeded in 6-well plates at 80% confluence and transfected with 2 μg per well of pGL3-basic and pGL3-E-cadherin-promoter, pGL3-basic and pGL3-Col1a1-promoter, and pGL3-basic and pGL3-miR-4739 vector. HEK293T cells were co-transfected with Smad1, Smad3 and Smad4 (2 μg) according to different groups. MeT-5A was treated with bleomycin, TGF-β1 or BMP-7 for 24 h according to the design. 2 μg RL-TK plasmid was used for transfection in each well. Cells were harvested after 24 h, and luciferase activity was measured using a dual-luciferase reporter assay system with a Synergy 2 Multi-Mode microplate reader. Relative expression of firefly and renilla luciferase was calculated.

2.17. Immunofluorescence staining of PMCs

To determine the intracellular localization of and changes in collagen-I, cytokeratin-8, vimentin, α-SMA, BMP-7, p-Smad2/3 and p-Smad1/5/9, PMCs were incubated with bleomycin (0.2 μg/ml) or/and BMP-7 (100 ng/ml) or both for 24 h. The cells were incubated with antibodies against collagen-I (dilution 1:50), cytokeratin-8 (dilution 1:50), vimentin (dilution 1:50), α-SMA (dilution 1:50), BMP-7 (dilution 1:50), p-Smad2/3 (dilution 1:30) and p-Smad1/5/9 (dilution 1:30) at 4 °C overnight. The Cy3-labeled secondary antibody IgG was added and incubated for 30 min. The nucleus was stained for DAPI for 10 min. Labeled cells were examined using a fluorescence microscope.

2.18. Human subjects

The study protocol was approved by the Institutional Review Board of the Tongji Medical College, Huazhong University of Science and Technology. Informed consent was obtained from all subjects. Human pleura slides were obtained from pleura biopsies of patients with tuberculous pleural effusion (TPE) or malignant pleural effusion (MPE). The criteria for TPE were the demonstration of granulomatous pleurisy in closed pleural biopsy specimen in the absence of any evidence of other granulomatous diseases. The criteria for MPE were the demonstration of cancerous cells in pleural fluid or in closed pleural biopsy specimen.

2.19. Immunofluorescence staining of human pleura samples

The human pleura slides were labeled for BMP-7 (dilution1:50) and counterstained using DAPI. The slides were mounted with anti-fade reagent and examined using the fluorescent microscope.

2.20. Immunofluorescence staining of mice pleura samples

The mice pleura slides were labeled for BMP-7 (dilution 1:50) and Wt1 (dilution 1:50) and counterstained using DAPI. The slides were mounted with anti-fade reagent and examined using the fluorescent microscope.

2.21. In situ hybridization histochemistry

To investigate miR-4739 levels in the pleura of human, in situ hybridization histochemistry was performed on the pleura tissues. The slides were incubated with hybridization buffer containing MK10483-miR-4739 probe (BOSTER, Wuhan, China) at 42 °C overnight. After added the blocking buffer, the slides were incubated with biotin-conjugated IgG fraction mouse anti-digoxin antibody, and subjected to streptavidin-biotin complex (SABC). Finally, the slides were undergoing chromogenic reaction with DAB kit.

2.22. Statistical analysis

In each cellular experiment, control and experimental cells were matched for cell line, age, seeding density, number of passages, and number of day post-confluence. Results are shown as the mean ± SEM. Differences between groups were analyzed using *t*-tests or ANOVA test. P values <0.05 were considered to be statistically significant.

3. Results

3.1. Bleomycin induces up-regulation of miR-4739 in human PMCs

To investigate miRNA expression alterations in PMCs, human PMCs (MeT-5A) were treated with bleomycin (0.2 μg/ml) for 24 h. RNA was isolated and the miRNA expression profile was analyzed. Heat-map and volcano-plot clearly revealed distinct expression patterns in some miRNAs in bleomycin-treated human PMCs compared to untreated control cells (Fig. 1a-b). As shown in Fig. 1b-c, bleomycin induced an increase in miR-4739 level compared to control. To further confirm bleomycin-induced change of miR-4739, miR-4739 PCR was performed in human PMCs. As shown in Fig. 1d, bleomycin increased the level of miR-4739 by 2.7 times compared to control.

3.2. TGF-β1 mediates bleomycin-induced up-regulation of miR-4739 by enhancing pri-miR-4739 promoter activity

To know what mediated bleomycin-indued up-regulation of miR-4739, we detected the level of TGF-β1 in human PMCs treated by bleomycin. As shown in Fig. 2a, bleomycin induced secretion of TGF-

β1 in human PMCs. Then human PMCs were directly treated with exogenous TGF-β1, and miR-4739 expression was investigated. We found exogenous TGF-β1 increased miR-4739 expression in human PMCs (Fig. 2b). SB431542 is an inhibitor of ALK5 (type I TGF-β receptor). As shown in Fig. 2c, bleomycin-induced up-regulation of miR-4739 in human PMCs, but this was blocked by SB431542. Based on the human genome assembly GRCh38, has-miR-4739 locates in the intergenic region. Intergenic miRNAs have their own promoters and transcription factors(TFs) [41]. So we hypothesized that up-regulation of miR-4739 was caused by TFs binding to promoter. According to miRTrans data [40], we chose two candidate TSSs and 1000 bp sequence before TSSs as potential promoters. Firstly, we chose the TSS located at chr 17: 79728551[−] which was 21,302 bp upstream of Pre-miRNA and cloned the 1000 bp before the TSS as promoter into pGL3-Basic, but the promoter had no activity (data not shown). Then, we detected the other TSS located at chr 17: 79741814[−] which was 34,565 bp upstream of the Pre-miRNA and cloned the 1000 bp before the TSS as promoter into pGL3-Basic, and its strong activity was confirmed both in HEK293T and human PMCs (Fig. 2d-f). Our previous study also showed that bleomycin activated Smad2/3 pathway in PMCs [37]. So we investigated the effect of Smad2/3 signaling on promoter activity of pri-miR-4739. As shown in Fig. 2d, mimicry of the Smad2/3 signaling increased pri-miR-4739 promoter activity in HEK293T. Moreover, bleomycin or TGF-β1 enhanced activation of the promoter of pri-miR-4739 in human PMCs (Fig. 2e-f). At same time, increased pri-miR-4739 levels were found in human PMCs treated with bleomycin or TGF-β1 compared with control (Fig. 2g-h). These data indicate that TGF-β1 mediates bleomycin-induced up-regulation of miR-4739 by enhancing the pri-miR-4739 promoter activity.

3.3. miR-4739 mediates MMT and collagen-I synthesis in PMCs

MMT in mesothelial cells is a key mechanism in fibrotic diseases. To investigate the role of up-regulated miR-4739 in pleural fibrosis, we detected MMT in PMCs. miR-4739 was up-regulated by employing a recombinant lentivirus in human PMCs (Fig. 3a), and miR-4739 overexpression increased protein levels of mesenchymal markers (α-SMA, vimentin) but decreased protein levels of mesothelial markers (E-cadherin, cytokeratin-8) (Fig. 3b). Moreover, Snail1, one marker of MMT was also increased. (Fig. S1a). At same time, miR-4739 overexpression induced collagen-I protein synthesis (Fig. 3b). Immunofluorescence staining also presented the same changes of these proteins in human PMCs (Fig. S2). Ability of proliferation and migration will increase when cells udergo MMT. Unsurprisingly, miR-4739 overexpression-induced cell proliferation and migration was found in human PMCs (Fig. 3c-e). To further confirm the role of miR-4739 in PMC-MMT, miR-4739 siRNA was used as miR-4739 inhibiton (Fig. S3a). As shown in Fig. S3b-c, bleomycin induced increases in mRNA and/or protein levels of collagen-I, α-SMA, vimentin and Snail1, and decreases in mRNA and/or protein levels of cytokeratin-8, E-cadherin in human PMCs. More importantly, miR-4739 inhibition prevented these changes (Fig. S1b and S3b-c). Bleomycin increaed the proliferation and migtarion abilities of PMCs, but these were also impeded by miR-4739 inhibition (Fig. S3d-e). All these data suggest that miR-4739 mediates MMT and collagen-I synthesis in PMCs, and high level miR-4739 promotes PMCs undergoing MMT and producing more collagen-I which contributes to fibrosis.

3.4. miR-4739 is high expression while BMP-7 is low expression in patients with pleural fibrosis

To further disclose the mechanism of miR-4739 mediating MMT, we made an endeavor to identify the target molecules of miR-4739 by using the TargetScan prediction software. The results indicated that BMP-7 is highly likely to be the target gene of miR-4739. Thus, we determined the levels of miR-4739 and BMP-7 in patients with pleural fibrosis. Positive expression of calretinin indicated a number of cells were PMCs in the clinical samples (Fig. 4a4-f4). Pleural fibrosis typically occurs following severe pleural inflammation. However, pleural fibrosis is very popular following tuberculous pleurisy, and seldom occurs after malignant pleurisy. As shown in Fig. 4a1-f1, Masson staining revealed that there were massive deposits of collagen (blue color) in the pleural sections from patients with tuberculous pleurisy (Fig. 4a1-c1). In malignant pleurisy, there was malignant tissue hyperplasia rather than pleural fibrosis with less collagen expressed (Fig. 4d1-f1). More importantly, higher level of miR-4739 (Fig. 4a2-c2) and lower level of BMP-7 (Fig. 4a3-c3) were found in tuberculous pleural fibrotic tissue compared to malignant pleural tissue (Fig. 4d2-f2 and Fig. 4 d3-f3). Pleural effusion often

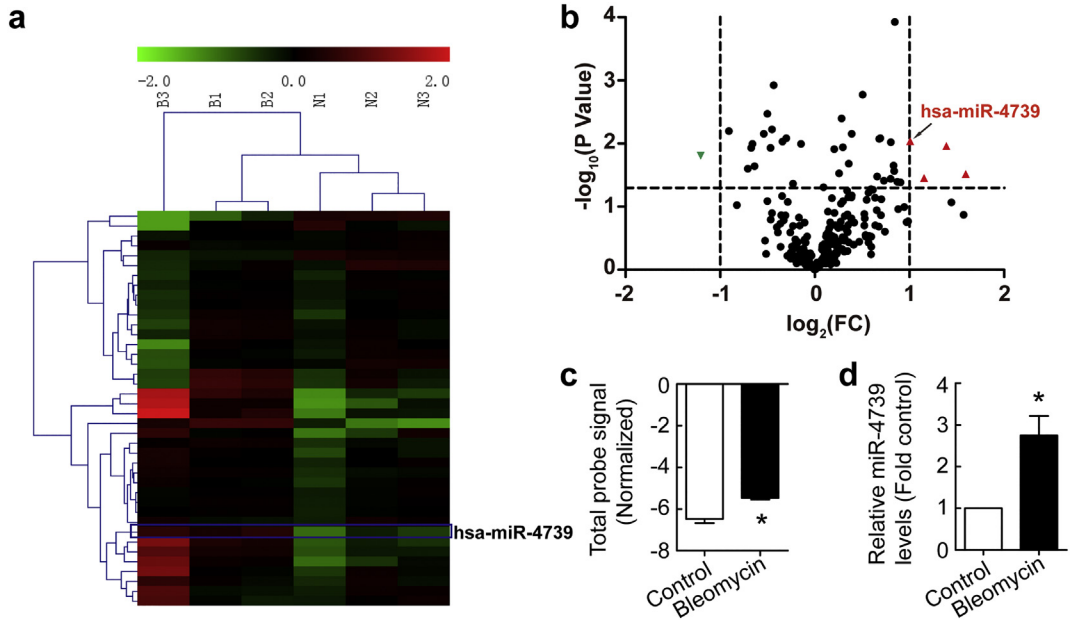

Fig. 1. Bleomycin induces up-regulation of miR-4739 in human PMCs. Human PMCs were treated with or without bleomycin (0.2 μg/ml) for 24 h after which miRNA expression profile assay and miR-4739 RT-qPCR were performed. (a) The heat map of miRNAs expression. (b) The volcano-plot of miRNAs expression. (c) Changes in miR-4739 level in miRNA microarray. n = 3, *P < 0.05 versus control (Student's *t*-test). (d) Changes in miR-4739 level investigated by using RT-qPCR. n = 4, *P < 0.05 versus control (Student's *t*-test).

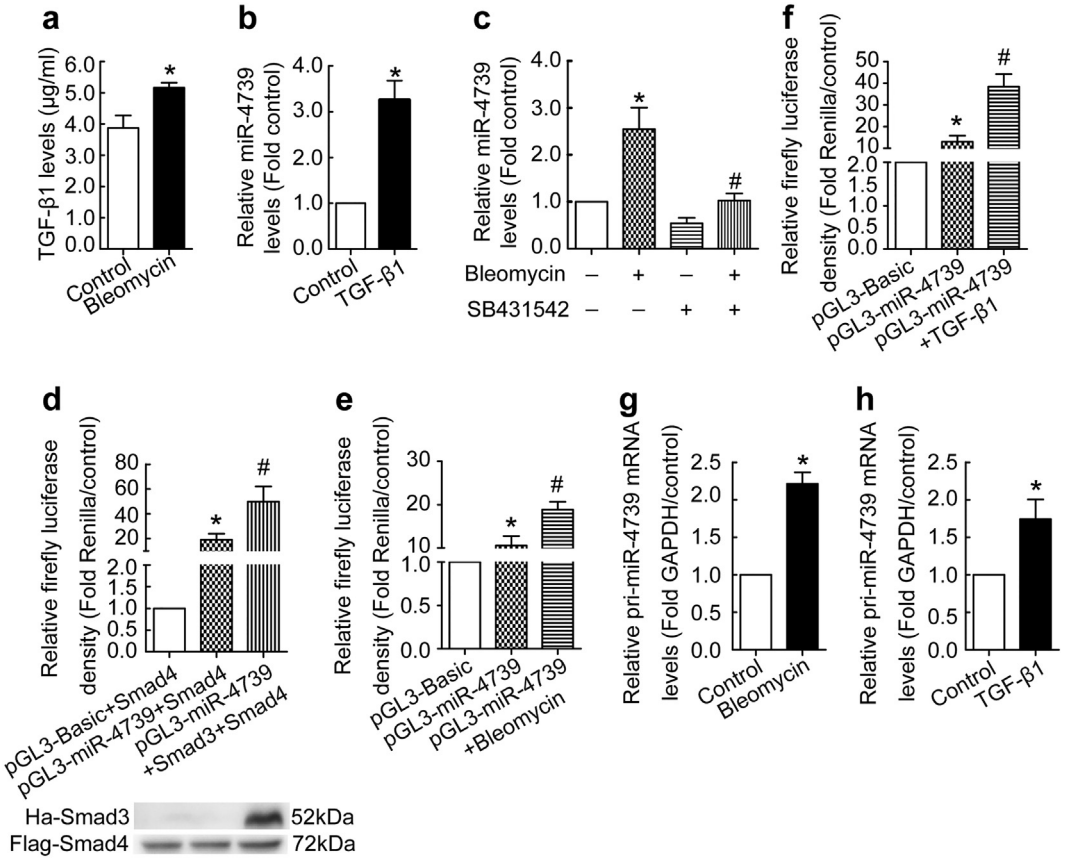

Fig. 2. TGF-β1 mediates bleomycin-induced up-regulation of miR-4739 by enhancing the pri-miR-4739 promoter activity. (a) Human PMCs were treated with or without bleomycin (0.2 μg/ml) for 24 h after which the levels of TGF-β1 in the cultured medium were detected by ELISA. n = 3, *P < 0.05 versus control (Student's *t*-test). (b) Human PMCs were treated with TGF-β1 (5 ng/ml) for 48 h after which miR-4739 RT-qPCR was performed. n = 8, *P < 0.05 versus control (Student's *t*-test). (c) Human PMCs were treated with bleomycin (0.2 μg/ml) with or without SB431542 (inhibitor of ALK5, type I TGF-β receptor) for 48 h. Then the levels of miR-4739 were detected by RT-qPCR. n = 6, *P < 0.05 versus control; #P < 0.05 versus bleomycin group (ANOVA test). (d) HEK 293 T cells were transfected with empty control vector or miR-4739 promoter plasmid, then the effect of Smad3 on pri-miR-4739 promoter was evaluated. All groups were transfected with Smad4 expression vector and a control renilla vector. n = 4, *P < 0.05 versus empty control vector; #P < 0.05 versus miR-4739 promoter plasmid (ANOVA test). (e-f) Human PMCs were transfected with miR-4739 promoter plasmid or empty control vector. After 24 h, the cells were treated with bleomycin (0.2 μg/ml) or TGF-β1 (0.5 ng/ml), the activity of the pri-miR-4739 promoter was detected. All groups were transfected with a control renilla expression. n = 4, *P < 0.05 versus empty control vector; #P < 0.05 versus miR-4739 promoter plasmid (ANOVA test). (g-h) Human PMCs were treated with 0.2 μg/ml bleomycin (g, n = 4) or 0.5 ng/ml TGF-β1 (h, n = 6) for 24 h, then the pri-miR-4739 level was detected. *P < 0.05 versus control (Student's *t*-test).

accompanies with tuberculous pleurisy and malignant pleurisy [42]. The human PMCs can break away from the pleura and suspend in the pleural effusion [43]. To further detect the miR-4739 and BMP-7 levels in clinic, we collected PMCs from patients with TPE and MPE (Fig. S4a). Higher level of miR-4739 and lower level of BMP-7 was found in PMCs from TPE of tuberculous pleurisy patients (Fig. S4b-c). Together, these results indicate that miR-4739 was markedly increased, but BMP-7 was significantly decreased in pleural tissue of patients with pleural fibrosis.

3.5. miR-4739 targets against BMP-7 and breaks the balance between Smad1/5/9 and Smad2/3 signaling

To further uncover the relationship between miR-4739 and BMP-7, we measured BMP-7 expression in human PMCs treated with miR-4739 over-expression. As shown in Fig. 5a, miR-4739 over-expression directly depressed expression of BMP-7 protein. On the other hand, bleomycin induced decreases of BMP-7, but miR-4739 inhibition restored the expression level of BMP-7 (Fig. 5b). To determine whether miR-4739 directly regulates BMP-7 gene expression, the binding ability of miR-4739 to the 3'UTR of BMP-7 gene was evaluated. Over-expression of miR-4739 significantly decreased the luciferase activity of the reporter vector containing wild 3'UTR (Fig. 5c). Point mutation in the 3'UTR of BMP-7 in the reporter vector abolished the decrease in the luciferase activity (Fig. 5c). BMP-7 belongs to TGF-β protein family and functioned through Smad1/5/9 pathway [29], thus p-Smad1/5/9 signaling was investigated. We found that miR-4739 over-expression inhibited p-Smad1/5/9 signaling in human PMCs (Fig. 5d). Bleomycin also depressed p-Smad1/5/9 expression, and this was blocked by miR-4739 inhibition (Fig. 5e). On the contrary, miR-4739 over-expression activated p-Smad2/3 signaling (Fig. 5d), while miR-4739 inhibition prevented bleomycin-induced increases of p-Smad2/3 (Fig. 5e). Interestingly, miR-4739 over-expression activated p-Smad2/3 signaling but the level of TGF-β1 did not change (Fig. S5). These data revealed that miR-4739 targets and down-regulates BMP-7, then breaks the balance between Smad1/5/9 and Smad2/3 signaling without TGF-β1 change.

To confirm the role of BMP-7-Smad1/5/9 in PMC-MMT, exogenous BMP-7 was used to treat human PMCs. As shown in Fig. 5f and S1c, bleomycin induced increases in collagen-I, α-SMA, vimentin and Snail1, decreases in *E*-cadhein and cytokeratin-8 in human PMCs. These changes were prevented by exogenous BMP-7. Moreover, exogenous BMP-7 also restored miR-4739 over-expression-mediated MMT in human PMCs (Fig. 5g and S1d). These results indicate that miR-4739 mediates PMC-MMT via BMP-7-Smad1/5/9 signaling.

3.6. BMP-7-Smad1/5/9 signaling regulates the promoter activity of E-cadherin and collagen-I genes

To furture clarify the mechanism of BMP-7 in PMC-MMT, we next studied Smad1/5/9-regulated gene promoter activity. As shown in

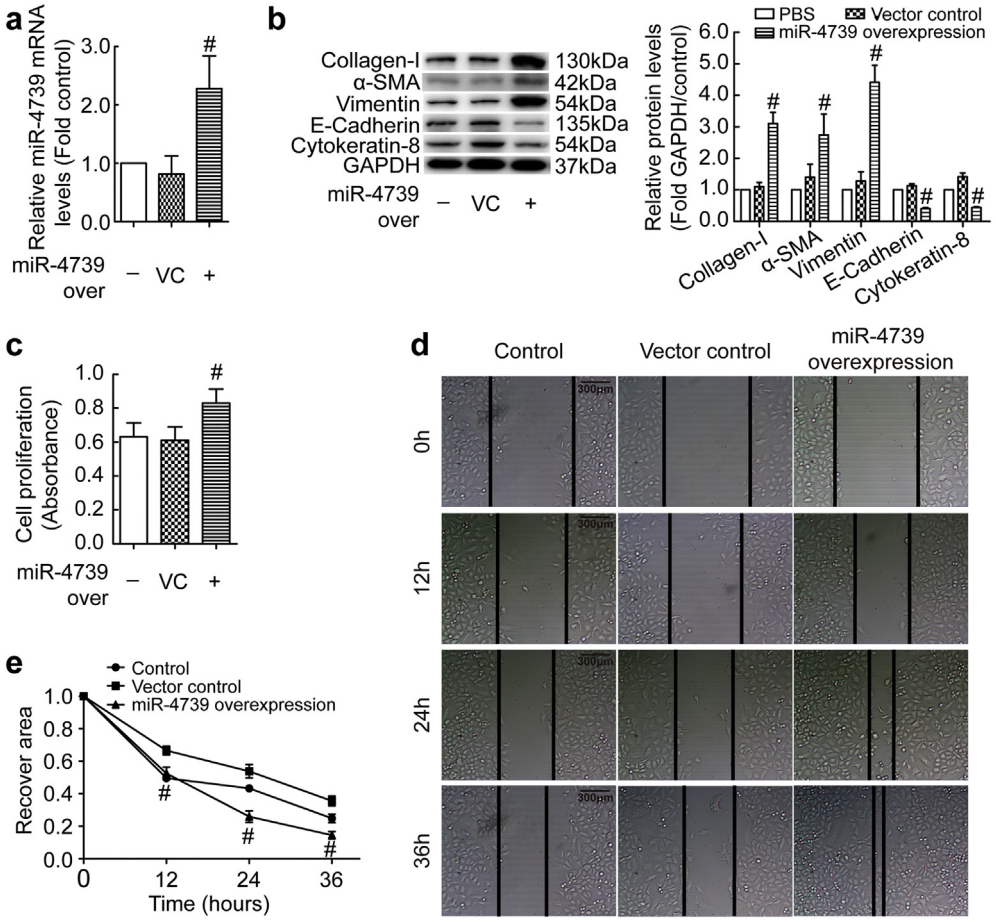

Fig. 3. miR-4739 mediates MMT and collagen-I synthesis in human PMCs. (a-c) Human PMCs were transducted with recombinant lentivirus vector containing miR-4739 or scrambled negative control (vector control) plasmids. (a) After 72 h, relative mRNA levels of miR-4739 were determined by RT-qPCR. n = 6, $^{\#}P < 0.05$ versus vector control (Student's *t*-test). (b) Changes of protein levels of collagen-I, α-SMA, vimentin, E-cadherin and cytokeratin-8 were measured by Western blotting after 96 h. n = 3, $^{\#}P < 0.05$ versus vector control (Student's *t*-test). (c) Changes in cell proliferation determined by CCK-8 kit after 72 h. n = 12, $^{\#}P < 0.05$ versus vector control (Student's *t*-test). (d-e) After 72 h, Representative image of cells migration and line graph depicting changes in recovery area in percentage of the initial scratched area. n = 5, $^{\#}P < 0.05$ versus vector control (Student's *t*-test).

Fig. S6a, BMP-7 prevented bleomycin-induced decreases of p-Smad1/5/9, and promoted p-Smad1/5/9 transferring into nucleus in human PMCs (Fig. S6b). Smad1, Smad2, Smad3, Smad5 and Smad9 belong to R-Smads which could interact with promoters to regulate transcription of target genes. These Smads could bind to gene promoter of E-cadherin which plays a pivotal role in triggering MMT [44]. Then we detected activity of E-cadherin promoter. As shown in Fig. S6c, mimicry of the Smad1/5/9 signaling increased the E-cadherin promoter activity which was decreased by Smad2/3 signaling in HEK293T. Moreover, in human PMCs, BMP-7 reversed TGF-β1-induced down-regulation of E-cadherin promoter activity as well as mRNA levels (Fig. S6d-e). On the contrary, mimicry of the Smad1/5/9 signaling decreased the Col1a1 (collagen-I encode gene) promoter activity which was increased by Smad2/3 signaling in HEK293T (Fig. S6f). TGF-β1 increased promoter activity and mRNA levels of collagen-I in human PMCs, and these were prevented by BMP-7 (Fig. S6 g-h). These results suggest that BMP-7-Smad1/5/9 signaling mediates PMC-MMT and collagen-I synthesis by regulating the promoter activity of E-cadherin and collagen-I genes.

3.7. miR-4739 over-expression results in pleural fibrosis in mice

We next explored whether miR-4739 could trigger pleural fibrosis in mice. However, no miR-4739 was found in the miRbase of mouse or rat, but BMP-7 of mouse or rat was highly homologous to human. Therefore, we attempted to detect the combining capacity of the miR-4739 with mouse or rat BMP-7. As shown in Fig. 6a, over-expression of miR-4739 was associated with significant decrease in luciferase activity when using a reporter vector containing wild-type mouse or rat BMP-7 3'UTR sequences. On the contrary, over-expression of miR-4739 didn't have inhibiting effect on luciferase activity with mutant mouse or rat BMP-7 3'UTR sequences. These results revealed miR-4739 could combine with mouse or rat BMP-7. To further identify the effect of miR-4739 in rat PMCs, we separated rat primary rat PMCs (Fig. S7a). As we expected, miR-4739 over-expression induced MMT in rat primary PMCs, and BMP-7 reversed the phenomenon through Smad1/5/9 signal pathway (Fig. 6b, S1e and S7b). Then we investigated the role of miR-4739 in mouse models. Just as description in the methods, lentivirus over-expression miR-4739, carbon particles or 0.9% NaCl was administrated in mice by intra-pleural injection. As shown in Fig. 6c-e, visceral pleura, parietal pleura and diaphragmatic pleura kept normal structures in the 0.9% NaCl treated mice. In the vector control group, carbon particles did not make changes in the pleura compared with 0.9% NaCl control mice. However, miR-4739 over-expression combined with carbon particles induced obvious pleural fibrosis in the visceral, parietal and diaphragmatic pleura. To further demonstrate that mouse pleural fibrosis was induced by miR-4739 targeting BMP-7, some miR-4739 over-expression mice were treated miR-4739 inhibition or BMP-7 by intra-pleural injection at days 11, 14 and 17. We found that the thickness of the pleura and the deposition of collagen significantly reduced in miR-4739 inhibition group (Fig. S8a-b) and BMP-7 group (Fig. S9a-b). Morover, the level of BMP-7 in PMCs was obviously reduced in miR-4739 over-expression mice (Fig. S8c), but when these mice were treated with miR-4739 inhibition, BMP-7 level was regained (Fig. S8c). These results indicate that miR-4739 exhibited defined function in

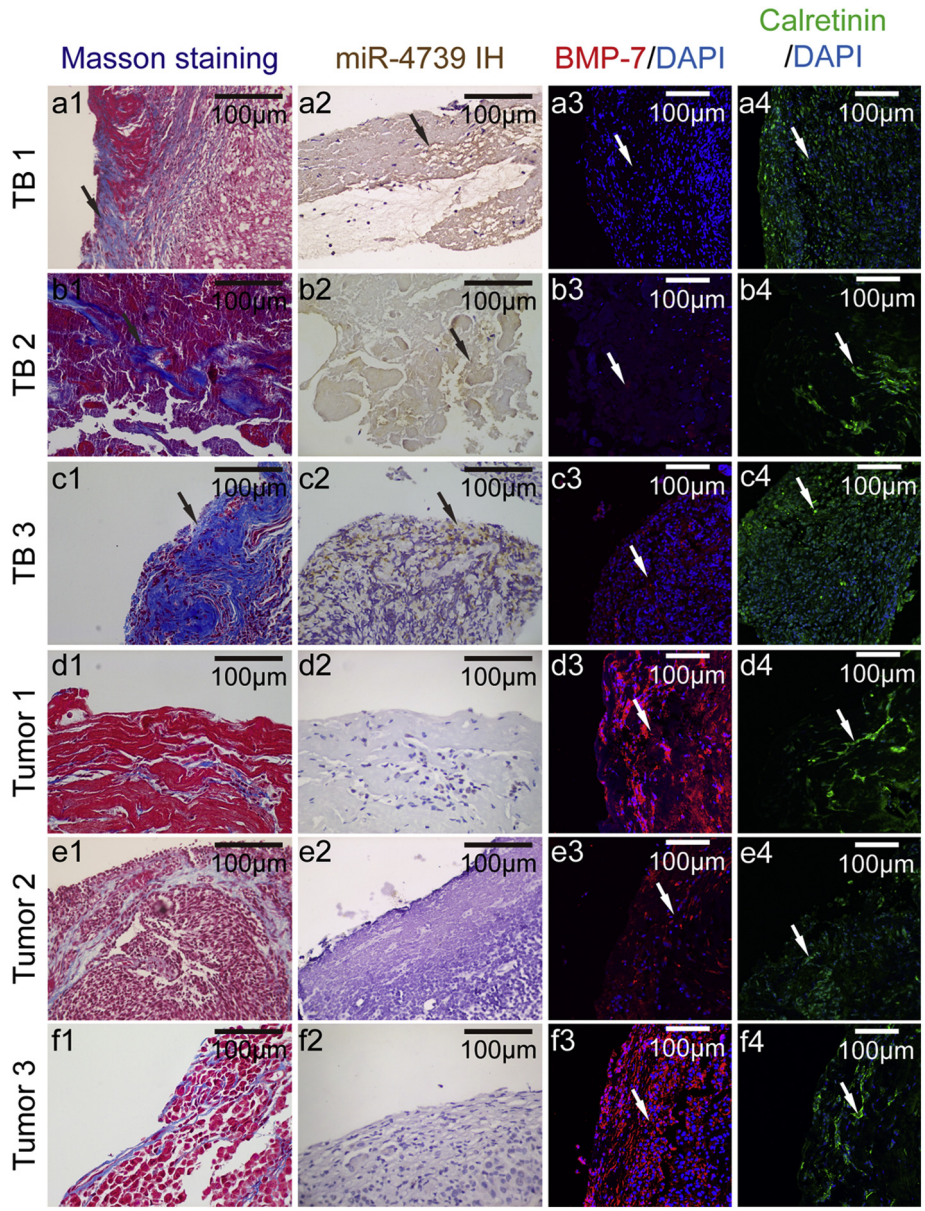

Fig. 4. miR-4739 is high but BMP-7 is low expressed in patients with pleural fibrosis. Pleural tissue samples were collected from parietal pleura in patients with TPE (TB1, 2, 3) or MPE (Tumor1, 2, 3). Pleura sections were stained with Masson's trichrome staining, in situ hybridization histochemistry and immunofluorescence staining. Blue color showed collagen in the Masson's trichrome stainings (a1-f1). In situ hybridization histochemistry stainings (a2-f2), yellow color showed miR-4739. Red color showed BMP-7 in immunofluorescence stainings (a3-f3). Green color showed calretinin in immunofluorescence staining (a4-f4).

promoting pleural fibrosis by targeting BMP-7 in mouse pleural fibrosis models.

3.8. BMP-7 reserved bleomycin induced pleural fibrosis in mice

Since miR-4739 over-expression induced pleural fibrosis in mice, whether changes in miR-4739-targeted-BMP-7 could reduce the pathological process. Therefore, we investigated the effect of BMP-7 in rat primary PMCs. Unsurprisingly, BMP-7 reserved bleomycin induced MMT and collagen-I synthesis through Smad1/5/9 and Smad2/3 pathway (Figs. 7a-b and S1f). Furthermore, in mouse models, bleomycin and carbon induced pleural fibrosis, while exogenous BMP-7 significantly alleviated visceral, parietal and diaphragmatic pleural fibrosis (Fig. 7c-e). These observations further indicate that miR-4739 targets against murine BMP-7 to trigger pleural fibrosis in vivo.

4. Discussion

In this study, we found that bleomycin-induced up-regulation of miR-4739 in PMCs. Then we identified that miR-4739-up-regulation was mediated by increased-TGF-β1 induced by bleomycin. miR-4739 over-expression induced MMT of PMCs, and miR-4739 inhibition prevented PMC-MMT. Investigation on the human specimens revealed that high levels of miR-4739 and low levels of BMP-7 associated with pleural fibrosis in patients. In the cells, it was confirmed that miR-4739 targeted and down-regulated BMP-7. Increased miR-4739 discouraged BMP-7/Smad1/5/9 signaling and activated Smad2/3 signaling which induced collagen-I synthesis in cells. Lastly, we demonstrated that miR-4739 over-expression induced pleural fibrosis, and exogenous BMP-7 prevented pleural fibrosis in mice. In a word, our data indicated that miR-4739 targets BMP-7 and mediates pleural fibrosis (Fig. 8), the miR-4739/BMP-7 axis is a promising therapeutic target.

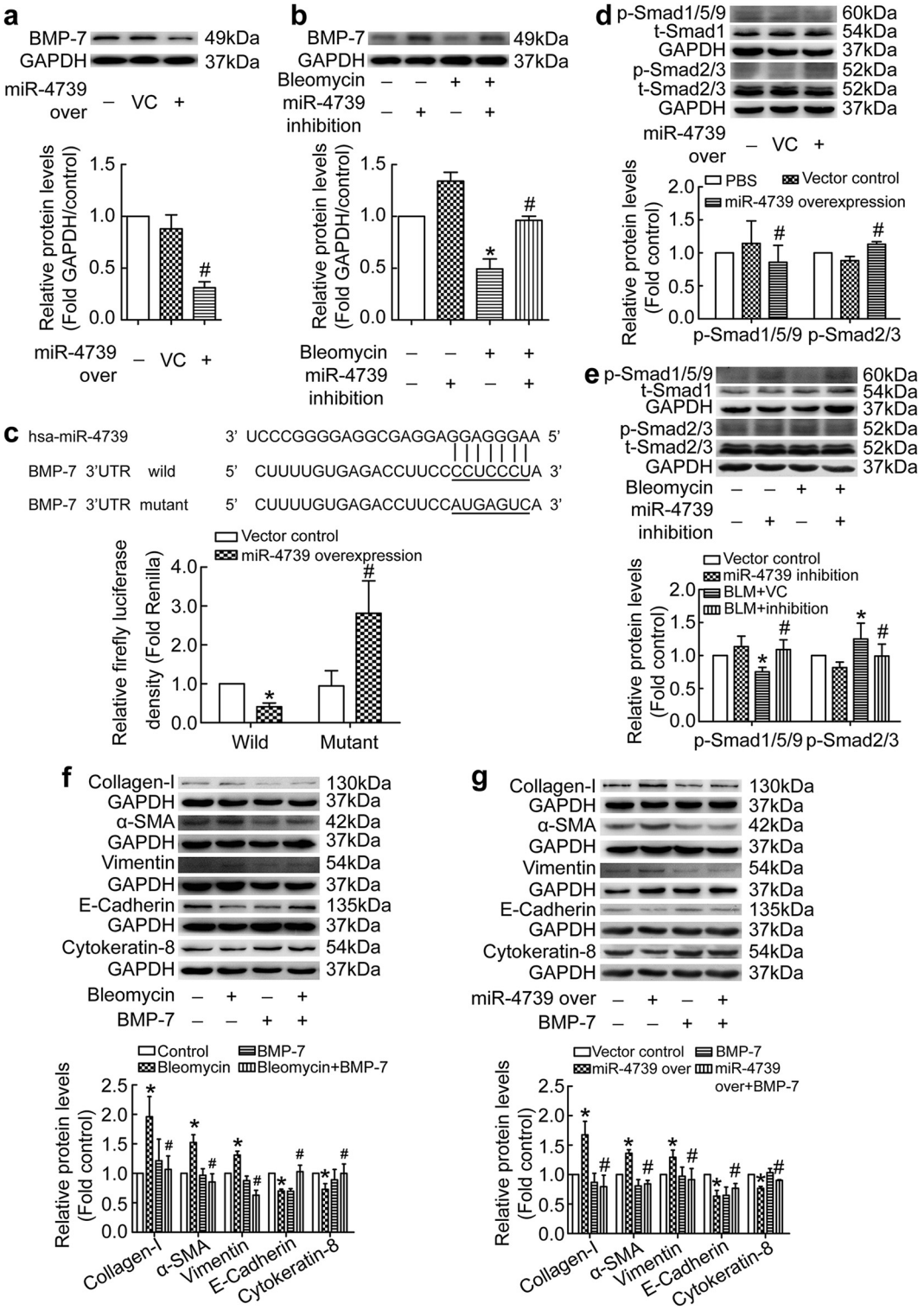

Fig. 5. miR-4739 targets against BMP-7 and breaks the balance between Smad1/5/9 and Smad2/3 signaling. (a) Human PMCs were transducted with recombinant lentivirus vector containing miR-4739 or scrambled negative control (vector control) plasmids. After 96 h, changes of BMP-7 protein levels measured by Western blotting. n = 3, $^{\#}P < 0.05$ versus vector control (Student's *t*-test). (b) Human PMCs were treated with bleomyin (0.2 μg/ml) for 24 h after transducted with recombinant lentivirus vector containing miR-4739-siRNA or control plasmids. BMP-7 was then detected by Western blotting. n = 3, $^{*}P < 0.05$ versus vector control, $^{\#}P < 0.05$ versus bleomycin group (ANOVA test). (c) Sequences of has-miR-4739 and the putative target sequence in the BMP-7 mRNA (wild-type) or an engineered mutant of this sequence (mutant) for the luciferase activity assay. n = 3, $^{*}P < 0.05$ versus wild-control; $^{\#}P < 0.05$ versus mutant-control (ANOVA test). (d) Human PMCs were ransducted with recombinant lentivirus vector containing miR-4739 or vector control. After 72 h, expressions of p-Smad1/5/9 (n = 6) and p-Smad2/3 (n = 4) were investigated by Western blotting. $^{\#}P < 0.05$ versus vector control (Student's *t*-test). (e) Human PMCs were treated as same as that in the b. Western blot analysis was used to evaluated protein levels of p-Smad1/5/9 (n = 4) and p-Smad2/3 (n = 10). $^{*}P < 0.05$ versus vector control, $^{\#}P < 0.05$ versus bleomycin group (ANOVA test). (f-g) Human PMCs were treated with bleomycin (0.2 μg/ml) or miR-4739 over-expression, and then exogenous BMP-7 was added (100 ng/ml). After 24 h, changes of protein levels of collagen-I (n = 5), α-SMA (n = 4), vimentin (f, n = 4; g, n = 8), E-cadherin (n = 4) and cytokeratin-8 (f, n = 5; g, n = 4) were investigated. $^{*}P < 0.05$ versus control, $^{\#}P < 0.05$ versus bleomycin group or miR-4739 over-expression group (ANOVA test).

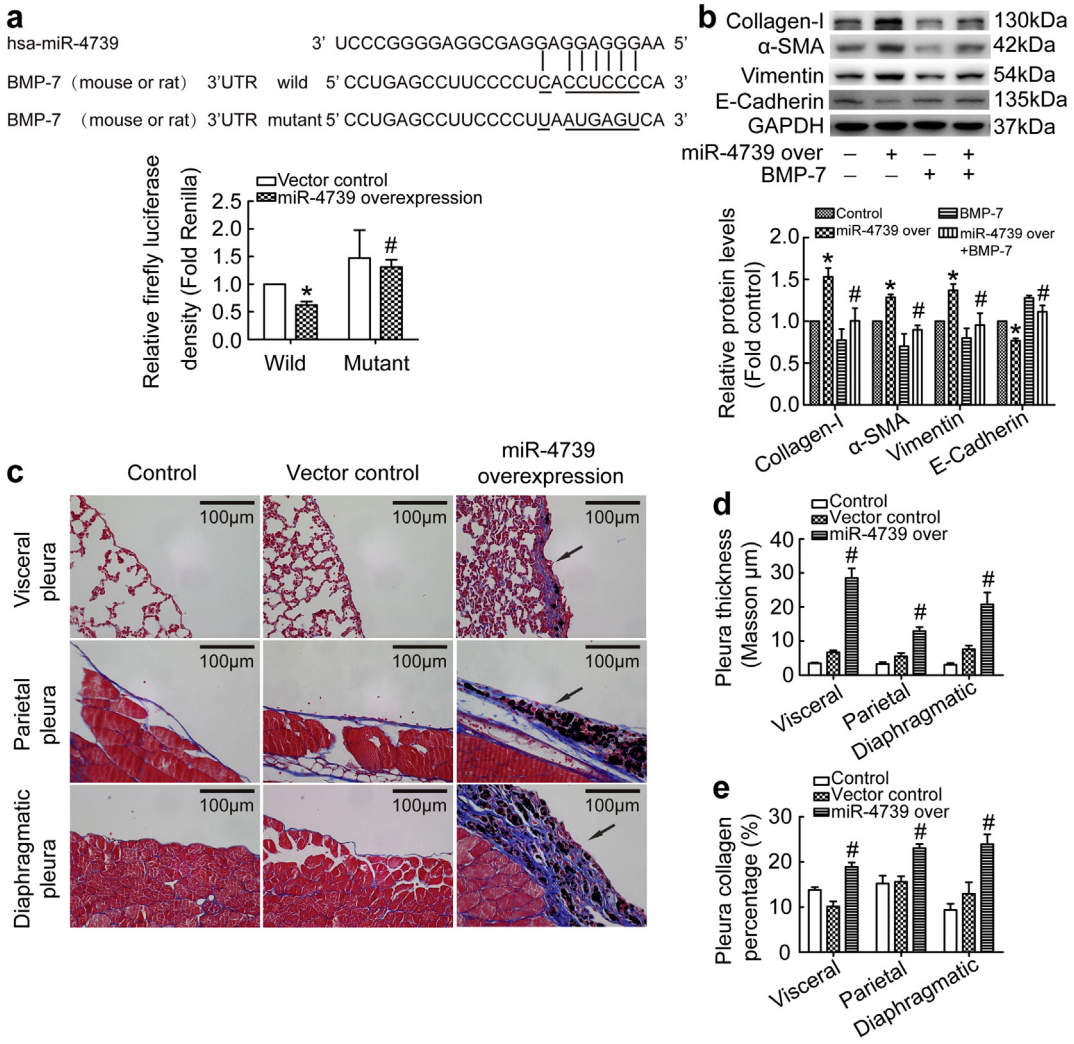

Fig. 6. miR-4739 over-expression results in pleural fibrosis in mice. (a) Sequences of has-miR-4739 and the putative target sequence in the mouse or rat BMP-7 mRNA (wild-type) or an engineered mutant of this sequence (mutant) for the luciferase activity assay. n = 3, *P < 0.05 versus wild-control; #P < 0.05 versus mutant-control (ANOVA test). (b) Rat primary PMCs were transducted with recombinant lentivirus vector containing miR-4739 or scrambled negativecontrol (vector control) plasmids, and then treated with or without BMP-7 (0.1 μg/ml) for 24 h. The protein levels of collagen-I, α-SMA, vimentin, and E-cadherin were detected. n = 3, *P < 0.05 versus vector control, #P < 0.05 versus miR-4739 over-expression group (ANOVA test). (c-e) C57BL/6 mice were treated with miR-4739 lentivirus plasmids or vector control lentivirus plasmids and carbon particles by intrapleural injection at days 1, 5 and 8. All mice were euthanized at day 21, and then tissues were taken for histological staining. (c) Masson's trichrome staining of visceral pleura, parietal pleura and diaphragmatic pleura. (d) Bar graphs depicting changes of pleura thickness. n = 3, #P < 0.05 versus vector control (Student's *t*-test). (e) Bar graphs depicting changes of pleura collagen percentage. n = 3, #P < 0.05 versus vector control (Student's *t*-test).

miRNAs play an important role in the posttranscriptional control of gene expression which is complicated in different physiological and pathophysiological processes including metabolism, growth, cell differentiation and development, apoptosis, inflammation and cell signaling [45]. The role of miRNA in pulmonary fibrosis and malignant pleural mesothelioma has been explored [46–50]. Brock and colleagues reported that low tissue levels of miR-125b predicted malignancy in solitary fibrous tumors of the pleura [51]. However, changes or regulatory effects of miRNAs in pleural fibrosis have not been revealed. Bleomycin is a classical inducer of fibrotic models including pulmonary and pleural fibrosis. In our present study, we treated PMCs with bleomycin and found the level of miR-4739 increased, and increased miR-4739 was mediated by TGF-β1. Recent studies revealed that PMCs undergoing MMT play a pivotal role in pleural and sub-pleural fibrosis [9,18,19]. Then we investigated the role of miR-4739 in PMC-MMT. miR-4739 over-expression induced PMC-MMT and miR-4739 inhibition prevented PMC-MMT which indicated that miR-4739 is an important regulator in PMC transition. PMCs undergoing MMT expressed high potential in cell migration and synthesis of collagen-I proteins which was involved in pleural fibrosis.

In order to clarify how miR-4739 regulates PMC-MMT and fibrosis, we investigated concerned signaling pathways. BMP-7 was highly likely to be the target gene of miR-4739 when using the TargetScan prediction software. Using clinical samples we exhibited miR-4739 over-expressed, and BMP-7 low-expressed in fibrotic pleura from patients. BMPs belong to the TGF-β protein family, and BMP-7 was considered as antagonist of organ fibrosis [52]. BMP-7 counteracts TGF-β1-induced EMT and attenuated fibrotic diseases including pulmonary, liver and renal fibrosis [31,53–55]. Loureiro et al reported that BMP-7 blocked MMT of mesothelial cells and prevented peritoneal damage induced by dialysis fluid exposure [56]. In the current study, we confirmed miR-4739 not only down-regulated BMP-7-Smad1/5/9 signaling but also activated Smad2/3 signaling pathway in human PMCs. However, miR-4739 did not change the levels of TGF-β1. So activation of Smad2/3 signaling should result from down-regulation of Smad1/5/9 not TGF-β1. Aykul and colleagues found that TGF-β family ligands could compete for Type II receptors and then causes different Smads signaling transduction [57]. Moreover, Smad1/5/9 and Smad2/3 maybe compete to bind with Smad4, because Smad4 is needed for both Smad1/5/9 and Smad2/3 to form compound which then moves into nucleus [58].

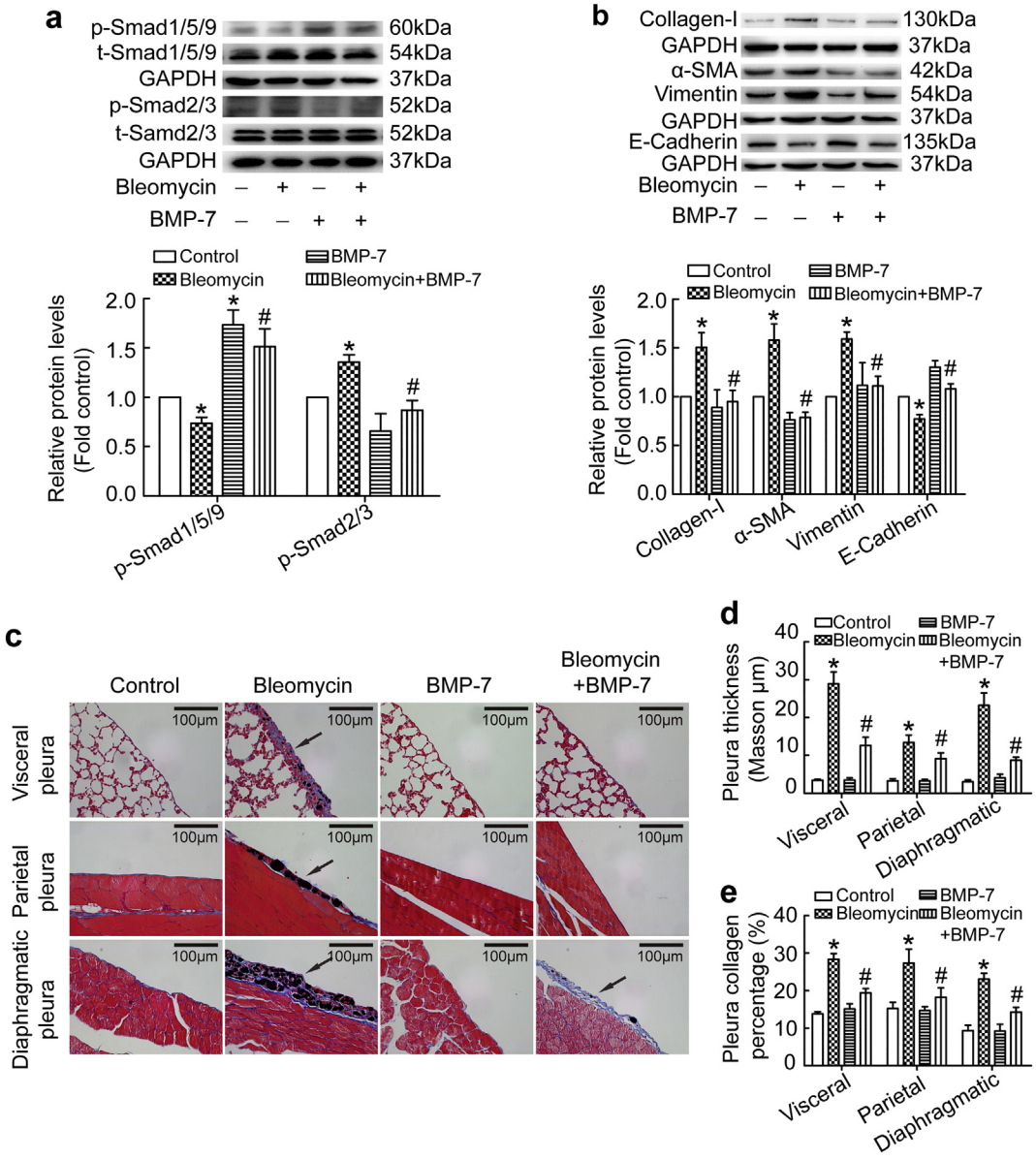

Fig. 7. BMP-7 reserved bleomycin induced pleural fibrosis in mice. (a-b) Rat primary PMCs were treated with or without bleomycin (0.2 μg/ml) in the presence or absence of BMP-7 (0.1 μg/ml) for 24 h. (a) Changes of protein levels of p-Smad2/3 and p-Smad1/5/9 were measured by Western blotting. n = 3, *P < 0.05 versus control, #P < 0.05 versus bleomycin group (ANOVA test). (b) Changes of protein levels of collagen-I (n = 4), E-cadherin (n = 3), vimentin (n = 3) and α-SMA (n = 4) were measured by Western blotting. *P < 0.05 versus control, #P < 0.05 versus bleomycin group (ANOVA test). (c-e) C57BL/6 mice were treated with a mixture of bleomycin and carbon particles or PBS by intrapleural injection. At days 4, 7 and 10, mice were treated with BMP-7 by intra-pleural injection. All mice were euthanized at day 21, and then tissues were taken for histological staining. (c) Masson's trichrome staining of visceral pleura, parietal pleura and diaphragmatic pleura. (d) Bar graphs depicting changes of pleura thickness. n = 4, *P < 0.05 versus control, #P < 0.05 versus bleomycin group (ANOVA test). (e) Bar graphs depicting changes of pleura collagen percentage. n = 4, *P < 0.05 versus control, #P < 0.05 versus bleomycin group (ANOVA test).

These should be the mechanism of interaction between Smad2/3 and Smad1/5/9 signaling in PMCs, which needs further investigation.

As a chemotherapeutics, bleomycin was found having side effects which one is inducing pulmonary fibrosis in the patients. In animal models, bleomycin is also an efficient and widely used compound for the induction of experimental pulmonary fibrosis [59]. However, it is difficult to generate pleural fibrosis in small rodents using bleomycin alone [35]. In 2010, Decologne and colleagues developed a mouse pleural fibrosis model by intra-pleural injection of bleomycin with carbon particles [35]. In their study, authors also confirmed neither bleomycin nor carbon particles can successfully induce pleural fibrosis. However, in our study, carbon particles exactly induced obvious pleural fibrosis in the presence of miR-4739 over-expression without bleomycin. In clinical practice, Talc is one of the most important factors which mediate pleural fibrosis by stimulating PMCs releasing active bFGF [60]. In our study, we found that bleomycin-induced fibrosis is likely mediated through TGF-β1. Thus, bleomycin with carbon particles induced model was used. Moreover, bleomycin with carbon particles induced mouse pleural fibrosis, and exogenous BMP-7 prevented pleural fibrosis in mice. Thus, using cell and animal models we revealed the role of miR-4739/BMP-7 in the plural fibrosis. It is also indicated that exogenous BMP-7 or miR-4739 inhibition prevents PMC-MMT and attenuates pleural fibrosis.

In summary, our findings provide evidences that bleomycin increases miR-4739 over-expression in PMCs. Over-expressed miR-4739 breaks the balance between Smad1/5/9 and Smad2/3 signaling pathway by targeting BMP-7 which mediated PMC-MMT and pleural fibrosis. Inhibition of miR-4739 might be a novel and promising approach in treatment of the disease.

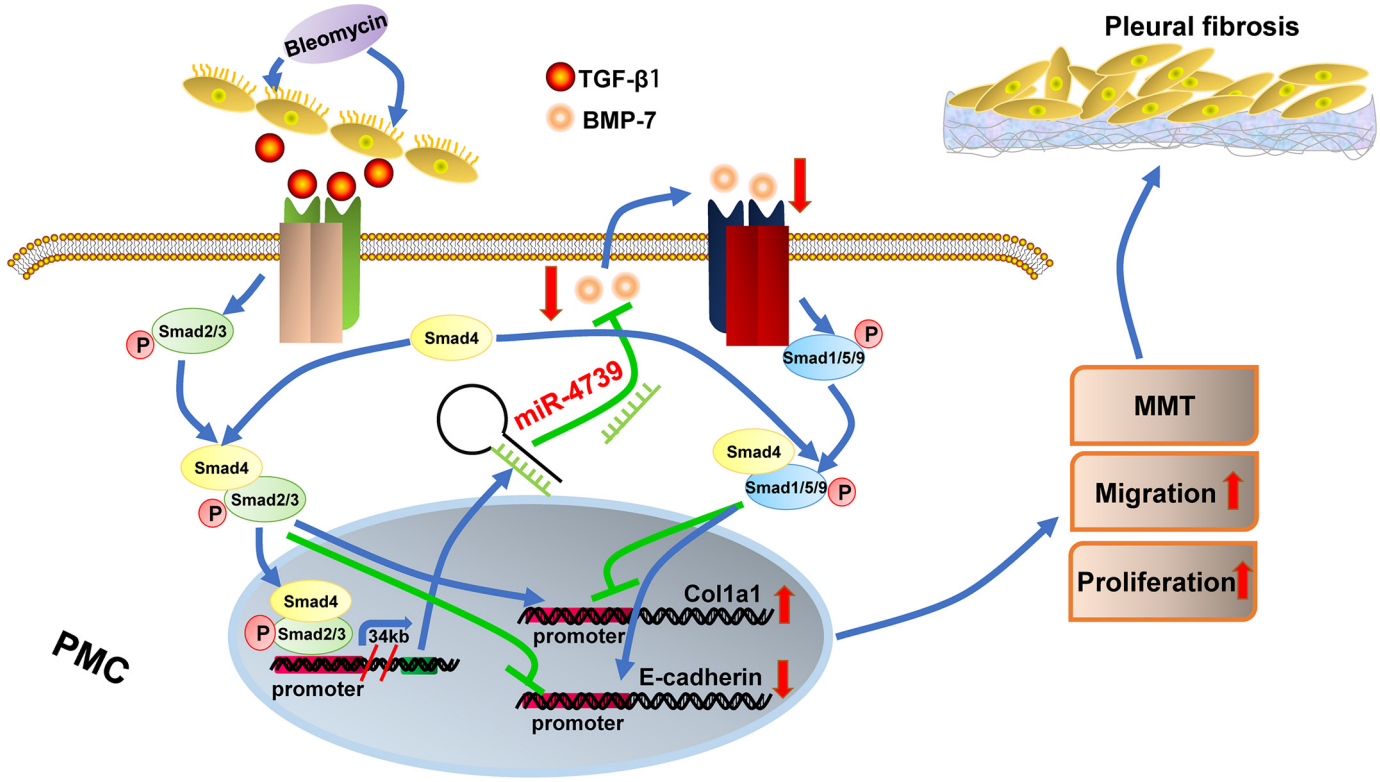

Fig. 8. miR-4739/BMP-7/Smad1/5/9 pathway induces pleural fibrosis. Bleomycin increased miR-4739 expression by activating Smad2/3 signaling. The up-expressed miR-4739 targeted and reduced BMP-7 expression which broke the balance between Smad1/5/9 and Smad2/3 signaling and led to pleural fibrosis.

Conflicts of interest

The authors declare no conflict of interest.

Author contributions statement

MW, LX, WLM and HY designed the study. MW, LX, LJJ, YZL, FL and LJS performed experiments. FX, XLH, FY and SYS analyzed the data. MW, WLM and HY wrote the manuscript. All authors have read and approved the manuscript.

Acknowledgements

This work was supported by the National Natural Science Foundation of China (No. 81600071, 81570087, 81873401, 81573485 and 91643101).

Appendix A. Supplementary data

Supplementary data to this article can be found online at https://doi.org/10.1016/j.ebiom.2019.02.057.

References

[1] Mutsaers SE, Prele CM, Brody AR, Idell S. Pathogenesis of pleural fibrosis. Respirology 2004;9(4):428–40.
[2] Batra H, Antony VB. Pleural mesothelial cells in pleural and lung diseases. J Thorac Dis 2015;7(6):964–80.
[3] Jantz MA, Antony VB. Pleural fibrosis. Clin Chest Med 2006;27(2):181–91.
[4] Huggins JT, Sahn SA. Causes and management of pleural fibrosis. Respirology 2004;9(4):441–7.
[5] Mutsaers SE. Mesothelial cells: their structure, function and role in serosal repair. Respirology 2002;7(3):171–91.
[6] Hillegass JM, Miller JM, MacPherson MB, Westbom CM, Sayan M, Thompson JK, et al. Asbestos and erionite prime and activate the NLRP3 inflammasome that stimulates autocrine cytokine release in human mesothelial cells. Part Fibre Toxicol 2013;10:39.
[7] Owens S, Jeffers A, Boren J, Tsukasaki Y, Koenig K, Ikebe M, et al. Mesomesenchymal transition of pleural mesothelial cells is PI3K and NF-kappaB dependent. Am J Physiol Lung Cell Mol Physiol 2015;308(12):L1265–73.
[8] Tucker T, Tsukasaki Y, Sakai T, Mitsuhashi S, Komatsu S, Jeffers A, et al. Myocardin is involved in Mesothelial-Mesenchymal transition of human pleural Mesothelial cells. Am J Respir Cell Mol Biol 2019. https://doi.org/10.1165/rcmb.2018-0121OC.
[9] Chen L-J, Ye H, Zhang Q, Li F-Z, Song L-J, Yang J, et al. Bleomycin induced epithelial-mesenchymal transition (EMT) in pleural mesothelial cells. Toxicol Appl Pharmacol 2015;283(2):75–82.
[10] Song L-J, Zhou L-L, Wang M, Liu F, Xiong L, Xiang F, et al. Lethal (2) giant larvae regulates pleural mesothelial cell polarity in pleural fibrosis. Biochim Biophys Acta Mol Cell Res 2018;1865(9):1201–10.
[11] Lagos-Quintana M, Rauhut R, Lendeckel W, Tuschl T. Identification of novel genes coding for small expressed RNAs. Science 2001;294(5543):853–8.
[12] Lau NC, Lim LP, Weinstein EG, Bartel DP. An abundant class of tiny RNAs with probable regulatory roles in Caenorhabditis elegans. Science 2001;294(5543):858–62.
[13] Lee RC, Ambros V. An extensive class of small RNAs in Caenorhabditis elegans. Science 2001;294(5543):862–4.
[14] Pandit KV, Corcoran D, Yousef H, Yarlagadda M, Tzouvelekis A, Gibson KF, et al. Inhibition and role of let-7d in idiopathic pulmonary fibrosis. Am J Respir Crit Care Med 2010;182(2):220–9.
[15] Bartis D, Mise N, Mahida RY, Eickelberg O, Thickett DR. Epithelial-mesenchymal transition in lung development and disease: does it exist and is it important? Thorax 2014;69(8):760–5.
[16] Willis BC, Borok Z. TGF-beta-induced EMT: mechanisms and implications for fibrotic lung disease. Am J Physiol Lung Cell Mol Physiol 2007;293(3):L525–34.
[17] Batra H, Antony VB. The pleural mesothelium in development and disease. Front Physiol 2014;5:284.
[18] Mubarak KK, Montes-Worboys A, Regev D, Nasreen N, Mohammed KA, Faruqi I, et al. Parenchymal trafficking of pleural mesothelial cells in idiopathic pulmonary fibrosis. Eur Respir J 2012;39(1):133–40.
[19] Nasreen N, Mohammed KA, Mubarak KK, Baz MA, Akindipe OA, Fernandez-Bussy S, et al. Pleural mesothelial cell transformation into myofibroblasts and haptotactic migration in response to TGF-beta1 in vitro. Am J Physiol Lung Cell Mol Physiol 2009;297(1):L115–24.
[20] Chen W, Ten Dijke P. Immunoregulation by members of the TGFbeta superfamily. Nat Rev Immunol 2016;16(12):723–40.
[21] Feng XH, Derynck R. Specificity and versatility in tgf-beta signaling through Smads. Annu Rev Cell Dev Biol 2005;21:659–93.
[22] Guasch G, Schober M, Pasolli HA, Conn EB, Polak L, Fuchs E. Loss of TGFbeta signaling destabilizes homeostasis and promotes squamous cell carcinomas in stratified epithelia. Cancer Cell 2007;12(4):313–27.

[23] Viloria-Petit AM, David L, Jia JY, Erdemir T, Bane AL, Pinnaduwage D, et al. A role for the TGFbeta-Par6 polarity pathway in breast cancer progression. Proc Natl Acad Sci U S A 2009;106(14033):14028–33.
[24] Paruchuri S, Yang JH, Aikawa E, Melero-Martin JM, Khan ZA, Loukogeorgakis S, et al. Human pulmonary valve progenitor cells exhibit endothelial/mesenchymal plasticity in response to vascular endothelial growth factor-a and transforming growth factor-beta2. Circ Res 2006;99(8):861–9.
[25] Heldin CH, Moustakas A. Signaling receptors for TGF-beta family members. Cold Spring Harb Perspect Biol 2016;8(8).
[26] Balli D, Ustiyan V, Zhang Y, Wang IC, Masino AJ, Ren X, et al. Foxm1 transcription factor is required for lung fibrosis and epithelial-to-mesenchymal transition. EMBO J 2013;32(2):231–44.
[27] Khalil H, Kanisicak O, Prasad V, Correll RN, Fu X, Schips T, et al. Fibroblast-specific TGF-beta-Smad2/3 signaling underlies cardiac fibrosis. J Clin Invest 2017;127(10):3770–83.
[28] Yang JW, Hien TT, Lim SC, Jun DW, Choi HS, Yoon JH, et al. Pin1 induction in the fibrotic liver and its roles in TGF-beta1 expression and Smad2/3 phosphorylation. J Hepatol 2014;60(6):1235–41.
[29] Chen D, Zhao M, Mundy GR. Bone morphogenetic proteins. Growth Factors 2004;22(4):233–41.
[30] Goumans MJ, Zwijsen A, Ten Dijke P, Bailly S. Bone morphogenetic proteins in vascular homeostasis and disease. Cold Spring Harb Perspect Biol 2018;10(2).
[31] Zeisberg M, Hanai J, Sugimoto H, Mammoto T, Charytan D, Strutz F, et al. BMP-7 counteracts TGF-beta1-induced epithelial-to-mesenchymal transition and reverses chronic renal injury. Nat Med 2003;9(7):964–8.
[32] Izumi N, Mizuguchi S, Inagaki Y, Saika S, Kawada N, Nakajima Y, et al. BMP-7 opposes TGF-beta1-mediated collagen induction in mouse pulmonary myofibroblasts through Id2. Am J Physiol Lung Cell Mol Physiol 2006;290(1):L120–6.
[33] Yao H, Ge T, Zhang Y, Li M, Yang S, Li H, et al. BMP7 antagonizes proliferative vitreoretinopathy through retinal pigment epithelial fibrosis in vivo and in vitro. FASEB J 2018:fj201800858RR. https://doi.org/10.1096/fj.201800858RR.
[34] Li X, Wang Y, An G, Liang D, Zhu Z, Lian X, et al. Bone marrow mesenchymal stem cells attenuate silica-induced pulmonary fibrosis via paracrine mechanisms. Toxicol Lett 2017;270:96–107.
[35] Decologne N, Wettstein G, Kolb M, Margetts P, Garrido C, Camus P, et al. Bleomycin induces pleural and subpleural fibrosis in the presence of carbon particles. Eur Respir J 2010;35(1):176–85.
[36] Yang J, Xiang F, Cai P-C, Lu Y-Z, Xu X-X, Yu F, et al. Activation of calpain by renin-angiotensin system in pleural mesothelial cells mediates tuberculous pleural fibrosis. Am J Physiol Lung Cell Mol Physiol 2016;311(1):L145–53.
[37] Zhang Q, Ye H, Xiang F, Song LJ, Zhou LL, Cai PC, et al. miR-18a-5p inhibits subpleural pulmonary fibrosis by targeting TGF-beta receptor II. Mol Ther 2017;25(3):728–38.
[38] Liu AD, Xu H, Gao YN, Luo DN, Li ZF, Voss C, et al. (Arg)9-SH2 superbinder: a novel promising anticancer therapy to melanoma by blocking phosphotyrosine signaling. J Exp Clin Cancer Res 2018;37(1):138.
[39] Deng J, Liu AD, Hou GQ, Zhang X, Ren K, Chen XZ, et al. N-acetylcysteine decreases malignant characteristics of glioblastoma cells by inhibiting notch2 signaling. J Exp Clin Cancer Res 2019;38(1):2.
[40] Hua X, Tang R, Xu X, Wang Z, Xu Q, Chen L, et al. mirTrans: a resource of transcriptional regulation on microRNAs for human cell lines. Nucleic Acids Res 2018;46(D1):D168–74.
[41] Monteys AM, Spengler RM, Wan J, Tecedor L, Lennox KA, Xing Y, et al. Structure and activity of putative intronic miRNA promoters. RNA 2010;16(3):495–505.
[42] Ohta Y, Shimizu Y, Matsumoto I, Watanabe G. Management of malignant pleural effusion by multimodality treatment including the use of paclitaxel administered by 24-hour intrathoracic infusion for patients with carcinomatous pleuritis. J Exp Clin Cancer Res 2006;25(1):15–9.
[43] Ye ZJ, Xu LL, Zhou Q, Cui A, Wang XJ, Zhai K, et al. Recruitment of IL-27-producing CD4(+) T cells and effect of IL-27 on pleural Mesothelial cells in Tuberculous pleurisy. Lung 2015;193(4):539–48.
[44] Karki S, Surolia R, Hock TD, Guroji P, Zolak JS, Duggal R, et al. Wilms' tumor 1 (Wt1) regulates pleural mesothelial cell plasticity and transition into myofibroblasts in idiopathic pulmonary fibrosis. FASEB J 2014;28(3):1122–31.
[45] Ebrahimi A, Sadroddiny E. MicroRNAs in lung diseases: recent findings and their pathophysiological implications. Pul Pharmacol Ther 2015;34:55–63.
[46] Njock MS, Guiot J, Henket MA, Nivelles O, Thiry M, Dequiedt F, et al. Sputum exosomes: promising biomarkers for idiopathic pulmonary fibrosis. Thorax 2018;74:309–12.
[47] Johnson TG, Schelch K, Cheng YY, Williams M, Sarun KH, Kirschner MB, et al. Dysregulated expression of the MicroRNA miR-137 and its target YBX1 contribute to the invasive characteristics of malignant pleural mesothelioma. J Thorac Oncol 2018;13(2):258–72.
[48] Cheng YY, Wright CM, Kirschner MB, Williams M, Sarun KH, Sytnyk V, et al. KCa1.1, a calcium-activated potassium channel subunit alpha 1, is targeted by miR-17-5p and modulates cell migration in malignant pleural mesothelioma. Mol Cancer 2016;15(1):44.
[49] Kurowska-Stolarska M, Hasoo MK, Welsh DJ, Stewart L, McIntyre D, Morton BE, et al. The role of microRNA-155/liver X receptor pathway in experimental and idiopathic pulmonary fibrosis. J Allergy Clin Immunol 2017;139(6):1946–56.
[50] Kao SC, Cheng YY, Williams M, Kirschner MB, Madore J, Lum T, et al. Tumor suppressor microRNAs contribute to the regulation of PD-L1 expression in malignant pleural mesothelioma. J Thorac Oncol 2017;12(9):1421–33.
[51] Brock M, Hottinger S, Diebold M, Soltermann A, Jochum W, Kohler M, et al. Low tissue levels of miR-125b predict malignancy in solitary fibrous tumors of the pleura. Respir Res 2017;18(1):43.
[52] Weiskirchen R, Meurer SK, Gressner OA, Herrmann J, Borkham-Kamphorst E, Gressner AM. BMP-7 as antagonist of organ fibrosis. Front Biosci 2009;14:4992–5012.
[53] Liang D, Wang Y, Zhu Z, Yang G, An G, Li X, et al. BMP-7 attenuated silica-induced pulmonary fibrosis through modulation of the balance between TGF-beta/Smad and BMP-7/Smad signaling pathway. Chem Biol Interact 2016;243:72–81.
[54] Weiskirchen R, Meurer SK. BMP-7 counteracting TGF-beta1 activities in organ fibrosis. Front Biosci 2013;18:1407–34.
[55] Zeisberg M, Yang C, Martino M, Duncan MB, Rieder F, Tanjore H, et al. Fibroblasts derive from hepatocytes in liver fibrosis via epithelial to mesenchymal transition. J Biol Chem 2007;282(32):23337–47.
[56] Loureiro J, Schilte M, Aguilera A, Albar-Vizcaino P, Ramirez-Huesca M, Perez-Lozano ML, et al. BMP-7 blocks mesenchymal conversion of mesothelial cells and prevents peritoneal damage induced by dialysis fluid exposure. Nephrol Dial Transplant 2010;25(4) (1098-108).
[57] Aykul S, Martinez-Hackert E. Transforming growth factor-beta family ligands can function as antagonists by competing for type II receptor binding. J Biol Chem 2016;291(20):10792–804.
[58] Wrana JL. Signaling by the TGFbeta superfamily. Cold Spring Harb Perspect Biol 2013;5(10):a011197.
[59] Mouratis MA, Aidinis V. Modeling pulmonary fibrosis with bleomycin. Curr Opin Pulm Med 2011;17(5):355–61.
[60] Antony VB, Nasreen N, Mohammed KA, Sriram PS, Frank W, Schoenfeld N, et al. Talc pleurodesis: basic fibroblast growth factor mediates pleural fibrosis. Chest 2004;126(5):1522–8.